Neutrino Coherent Scattering Rates at Direct Dark Matter Detectors

Louis E. Strigari

Kavli Institute for Particle Astrophysics and Cosmology, Stanford University, Stanford, CA 94305, USA

E-mail: `strigari@stanford.edu`

Abstract. Neutrino-induced recoil events may constitute a background to direct dark matter searches, particularly for those detectors that strive to reach the ton-scale and beyond. This paper discusses the expected neutrino-induced background spectrum due to several of the most important sources, including solar, atmospheric, and diffuse supernova neutrinos. The largest rate arises from ^{8}B produced solar neutrinos, providing upwards of $\sim 10^3$ events per ton-year over all recoil energies for the heaviest nuclear targets. However the majority of these ^{8}B events are expected to be below the recoil threshold of modern detectors. The remaining neutrino sources are found to constitute a background to the WIMP-induced recoil rate only if the WIMP-nucleon cross section is less than 10^{-12} pb. Finally the sensitivity to diffuse supernova neutrino flux for non-electron neutrino flavors is discussed, and projected flux limits are compared with existing flux limits.

1. Introduction

Weakly-Interacting Massive Particles (WIMPs) are a leading candidate for the dark matter that constitutes $\sim 23\%$ of the mass density of the Universe [1]. A promising means to search for WIMPs is through direct interactions in underground detectors, whereby the struck nucleus recoils coherently and its kinetic energy is deposited into scintillation light. At the present, detectors constrain the spin-independent WIMP-nucleon cross section to be $\lesssim 9 \times 10^{-44}$ cm^2 for WIMPs in the mass range $\lesssim 100$ GeV [2, 3]. Future detectors are expected to reach the ton-scale and beyond, providing the exciting prospect of covering much of the model parameter space for leading dark matter candidates [4].

Present direct detection experiments report upper limits on the WIMP mass and cross section under the assumption of unknown backgrounds [5]. As the sizes of these detectors continue to increase, backgrounds that are beyond the sensitivity limit of modern detectors will reveal themselves, necessitating a detailed understanding of these background spectra and new techniques for their reduction. Due to the nature of the detected events, background subtraction requires understanding the rate and spectral shape of any signal that leads to a coherent nuclear recoil event in the energy window where a dark matter signal appears.

In his seminal work over thirty years ago, Freedman [6] pointed out that the neutrino-nucleon neutral current interaction leads to a coherence effect, whereby the neutrino-nucleus elastic scattering cross section is enhanced and scales approximately as the square of the number of neutrons in the nucleus. Coherent recoils are expected if the three-momentum imparted to the nucleus, q, obeys the inequality $qR \lesssim 1$, where R is the radius of the nucleus. For typical nuclear radii, coherent scattering leads to nuclear recoils in the range of a few keV for incoming neutrinos with energies in the range $\sim 1 - 100$ MeV. Though neutrino-nucleus coherent scattering remains a fundamental prediction of the Standard Model, this process has yet to be observed experimentally [7].

Solar, atmospheric, and reactor neutrinos may induce observable nuclear recoil events [8]. Monroe and Fisher [9] have recently determined the coherent scattering rates in future dark matter detectors due to solar, atmospheric, and geo-neutrinos, in particular identifying ^{8}B solar neutrinos as the source with the largest event rate. For detectors at the $\sim$ ton-yr exposure scale, ^{8}B neutrino-induced recoils are significant for recoil energies $\lesssim 3$ keV for heavy targets such as Xe and $\lesssim 30$ keV for lighter targets such as Flourine and Carbon. Assuming a ~ 100 GeV WIMP, ^{8}B neutrino-induced recoils constitute a background to the WIMP recoil spectrum if the WIMP-nucleon cross section is $\lesssim 10^{-10}$ pb [9, 10].

The goal of this paper is to provide a survey of the expected event rate recoil spectra from several important astrophysical neutrino sources. Solar, atmospheric, and diffuse supernova neutrinos are studied; geo-neutrinos are not considered since their signal is dwarfed by the solar neutrino signal over a similar energy range [9]. In addition to providing an updated calculation of the solar and atmospheric neutrino fluxes for

a variety of often-discussed nuclear targets, the first predictions for the recoil energy spectrum of the *Diffuse Supernova Neutrino Background (DSNB)* are provided. If the ^{8}B neutrinos can be fit, or if the dominant component to their recoil spectrum lies below the analysis energy threshold, astrophysical neutrino backgrounds will only contaminate a WIMP-nucleon recoil signal if the WIMP-nucleon cross section is $\lesssim 10^{-12}$ pb. It is additionally shown that, with current exposures, detectors should have sensitivity to reduce the current upper limit on the ν_μ and ν_τ component of *DSNB* flux by more than an order of magnitude.

2. Neutrino-Induced Recoil Spectra

2.1. Neutrino-Nucleus Coherent Scattering

The neutrino-nucleus scattering cross section per recoil kinetic energy T is [11]

$$\frac{d\sigma(E_\nu, T)}{dT} = \frac{G_f^2}{4\pi} Q_w^2 M \left(1 - \frac{MT}{2E_\nu^2}\right) F(Q^2)^2. \tag{1}$$

Here $Q_w = N - (1 - 4\sin^2\theta_w)Z$ is the weak nuclear charge, where N is the number of neutrons and Z is the number of protons. The mass of the nucleus is $M = AM_N$, where $A = N + Z$ is the mass number and $M_N = 931$ MeV. From kinematics the recoil energy is related to the neutrino three-momentum via $q^2 = 2MT$, and the maximum three-momentum transfer is a function of the neutrino energy, $q_{max}^2 = 4E_\nu^2$. The range of recoil energy for the struck nucleus varies between 0 and $T_{\max}$, where

$$T_{\max} = \frac{2E_\nu^2}{M + 2E_\nu}. \tag{2}$$

Taking the limit $M \gg 2E_\nu$, which will always be valid for the results presented here, the minimum neutrino energy for a fixed recoil kinetic energy T is $E_\nu = \sqrt{MT/2}$.

The form factor, $F(Q^2)^2$, is a function of the 4-momentum, Q, and measures the distribution of nucleons within the nucleus and thus the deviations from coherence at high recoil energies, defined by momentum transfers $qR \gtrsim 1$. The form factor at zero momentum transfer scales as $F(0)^2 \to 1$ for $qR \ll 1$. To approximate the effects of the form factor, the analysis in this paper uses the Helm form factor as parametrized in Lewin and Smith [12]. As in the case of WIMP-nucleon recoils, the form factor has the primary effect of reducing the cross section for large momentum transfers.

2.2. Neutrino Fluxes

Since the coherent scattering process is "flavor blind," mixing angles which connect neutrino weak flavor eigenstates to mass eigenstates need not be considered in flux calculations. For all of the sources, the energy spectrum for the weak flavor eigenstates at the production sites are used.

Solar Neutrinos - The calculations in this paper consider two sources of solar neutrinos, so-called ^{8}B and *hep* neutrinos. These neutrinos come from the reactions

^{8}B $\rightarrow$ ^{7}Be* + e^+ + ν_e and ^{3}He +p $\rightarrow$^{4}He +e^+ + ν_e, which occur in $2 \times 10^{-2}\%$ and $2 \times 10^{-5}\%$ of the terminations of the solar pp chain, respectively [13]. The remaining sources of solar neutrinos induce recoils with energies and rates below that of the ^{8}B induced spectrum. For example, neutrinos produced directly in the pp reaction only induce recoils up to a maximum kinetic energy of ~ 0.03 keV [9].

Atmospheric Neutrinos– Cosmic ray collisions in the atmosphere produce a primary flux of ν_e, $\bar{\nu}_e$, ν_μ, and $\bar{\nu}_\mu$ [14], with a spectrum that extends up to energies of ~ 100 GeV. At these high energies, the loss of coherence in the scatterings must be accounted for. On the one hand, the coherent scattering cross section scales as the neutrino energy squared, favoring high neutrino energies. On the other hand, the form factor suppresses scatterings for high momentum transfers, which largely result from the highest energy neutrinos in the flux distribution. Convolving both of these factors means that detectors are mainly sensitive to the atmospheric neutrino flux $\lesssim 100$ MeV. A more exact upper cut-off depends on the detector target; the larger the mass number of the nucleus, the more strongly the event rate is suppressed by the form factor at the highest detectable recoil energies. For the atmospheric neutrino flux, the calculations in this paper use the published Fluka results for the Kamioka location, which have been determined down to neutrino energies ~ 10 MeV [15]. At energies of interest for this calculation, $\lesssim 100$ MeV, there is a $\sim 20\%$ uncertainty in the normalization of the flux, primarily due to geo-magnetic effects.

Diffuse Supernova Neutrinos- Core-collapse supernova produce a burst of $\sim 10^{58}$ neutrinos of all flavors per explosion; the past history of all of these explosions produce a *Diffuse Supenova Neutrino Background (DSNB)*. The *DSNB* flux is a convolution of the core-collapse supernova rate as a function of redshift with the neutrino spectrum per supernova. The core-collapse rate is derived from the star-formation rate and stellar initial mass function; the calculations in the paper follow the recent results of Horiuchi et al. [16]. The neutrino spectrum of a core-collapse supernova is believed to be similar to a Fermi-Dirac spectrum, with temperatures in the range 3-8 MeV [17]. The calculations in this paper assume the following temperatures for each neutrino flavor: $T_{\nu_e} = 3$ MeV, $T_{\bar{\nu}_e} = 5$ MeV, and $T_{\nu_x} = 8$ MeV. Here T_{ν_x} represent the four flavors ν_μ, $\bar{\nu}_\mu$, ν_τ, and $\bar{\nu}_\tau$. Due to the $\sim E_\nu^2$ scaling of the total cross-section in Eq. 1 (integrated over all recoil energies), the flavors with the largest temperature dominate the event rate.

There are strong upper limits on the $\bar{\nu}_e$ component of the *DSNB* flux from Super-Kamiokande, < 1.2 cm^{-2} s^{-1} [18]. This flux limit constrains the high energy tail of the *DSNB* flux, specifically neutrino energies $\gtrsim 18$ MeV. More recently, the SNO collaboration has placed an upper limit on the ν_e component of the flux of ~ 70 cm^{-2} s^{-1} for neutrinos in the energy range of $22.9 - 36.9$ MeV [19]. Though weaker than the $\bar{\nu}_e$ limit, the SNO ν_e limit does probe the parameter space for exotic core-collapse models [20]. An indirect bound on the ν_e flux that rivals the present limit on the $\bar{\nu}_e$ flux follows from oscillation conditions [21], and stronger direct bounds on the ν_e flux may be realized in future Argon TPC detectors [22]. The strongest bound on ν_x flavors comes from the Mt. Blanc experiment [23], which quotes an upper limit on the ν_x flux of $\sim 10^7$

cm^{-2} s^{-1} for neutrino energies $\gtrsim 20$ MeV. This flux limit was set based on the neutral current interaction with ^{12}C. It has additionally been proposed that Super-Kamiokande can set an improved limit on the ν_x flux [24]. Below the prospects for improving on these ν_x flux limits are discussed.

In addition to the *DSNB*, detectors sensitive to low energy nuclear recoils may be used to detect a supernova burst in the Galaxy [25]. For exposures on the scale of $\sim$ ton-yr, there are expected to be of order 10 events, summed over all flavors for a supernova at 10 kpc [26]. The detection of a supernova burst via a recoiling nucleus would provide a unique window into supernova physics, complementing the detection of proton recoils [27] as the best means to study the ν_x component of the neutrino flux.

Figure 1 shows the neutrino flux spectra for solar, atmospheric, and *DSNB* sources. In terms of integrated flux, the ^{8}B flux is by far dominant, nearly three orders of magnitude larger than the next closest *hep* rate. However, as the ^{8}B flux is confined to energies $\lesssim 16$ MeV, these will produce lower energy recoils in comparison to the higher energy *DSNB* and atmospheric components. A convolution between the flux and cross section is required to obtain the recoil rate as a function of energy; the goal of the following section is to determine these respective rates.
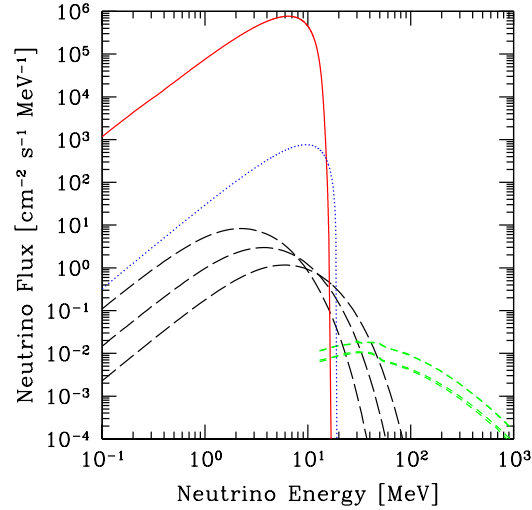

Figure 1. Neutrino fluxes for astrophysical sources that constitute the dominant backgrounds to WIMP recoil signals. From top to bottom on the left, the fluxes are solar ^{8}B (solid, red) and *hep* (dotted, blue), *DSNB* (long-dash, black) with temperatures of 3 5, and 8 MeV (corresponding to ν_e, $\bar{\nu}_e$, and ν_x, respectively, where ν_x symbolizes muon and tau neutrinos and the respective antiparticles). The short-dashed (green) curves at the highest energies are the atmospheric neutrino fluxes, plotted down to the lowest energy in the calculation of Ref. [15]. From bottom to top on the right, the fluxes are for ν_e, $\bar{\nu}_e$, then ν_μ, $\bar{\nu}_\mu$.
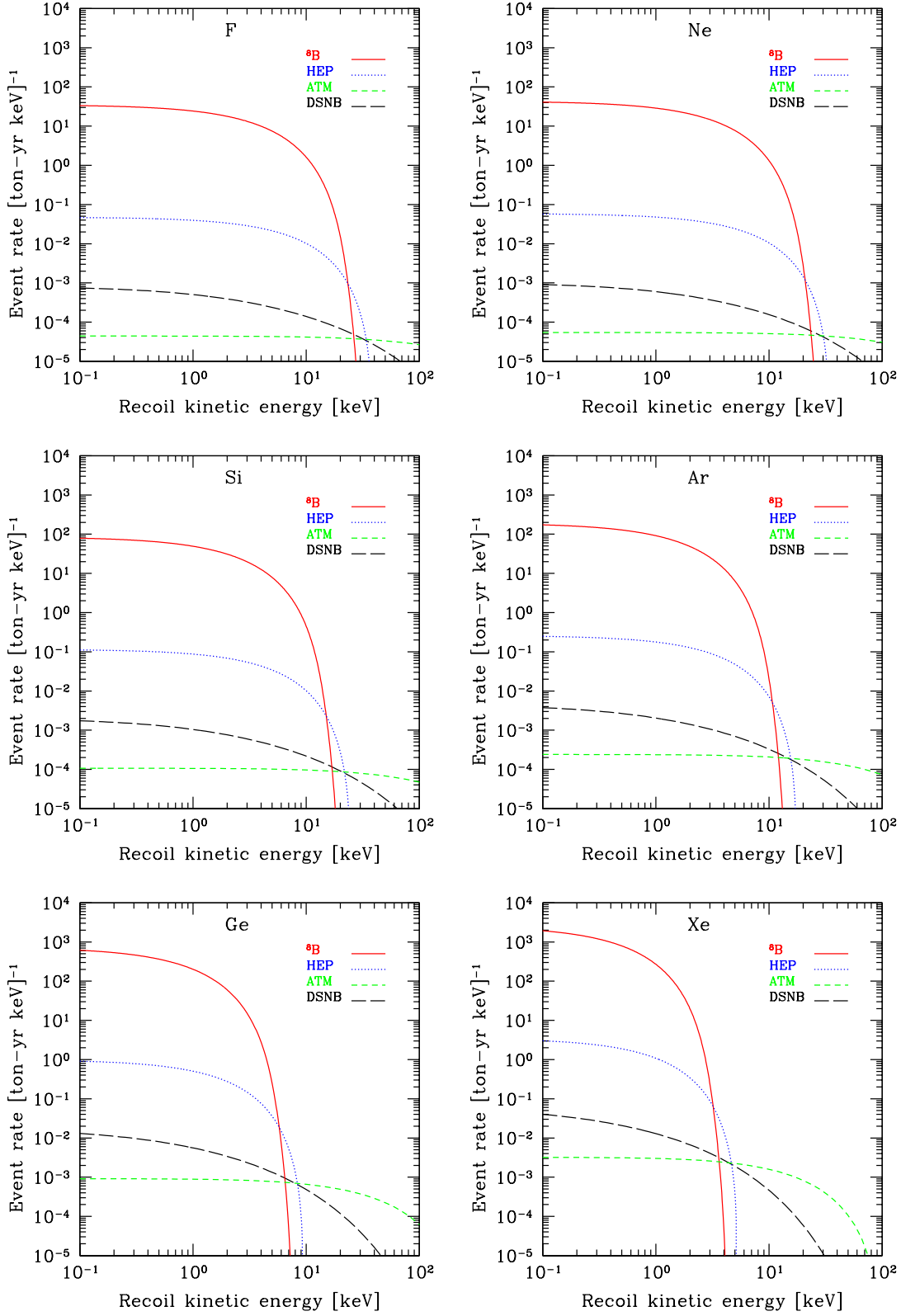
Figure 2. Event rate per recoil kinetic energy for six target nuclei. For both the diffuse supernova and atmospheric event rates, the sum of all contributing neutrino flavors are shown.
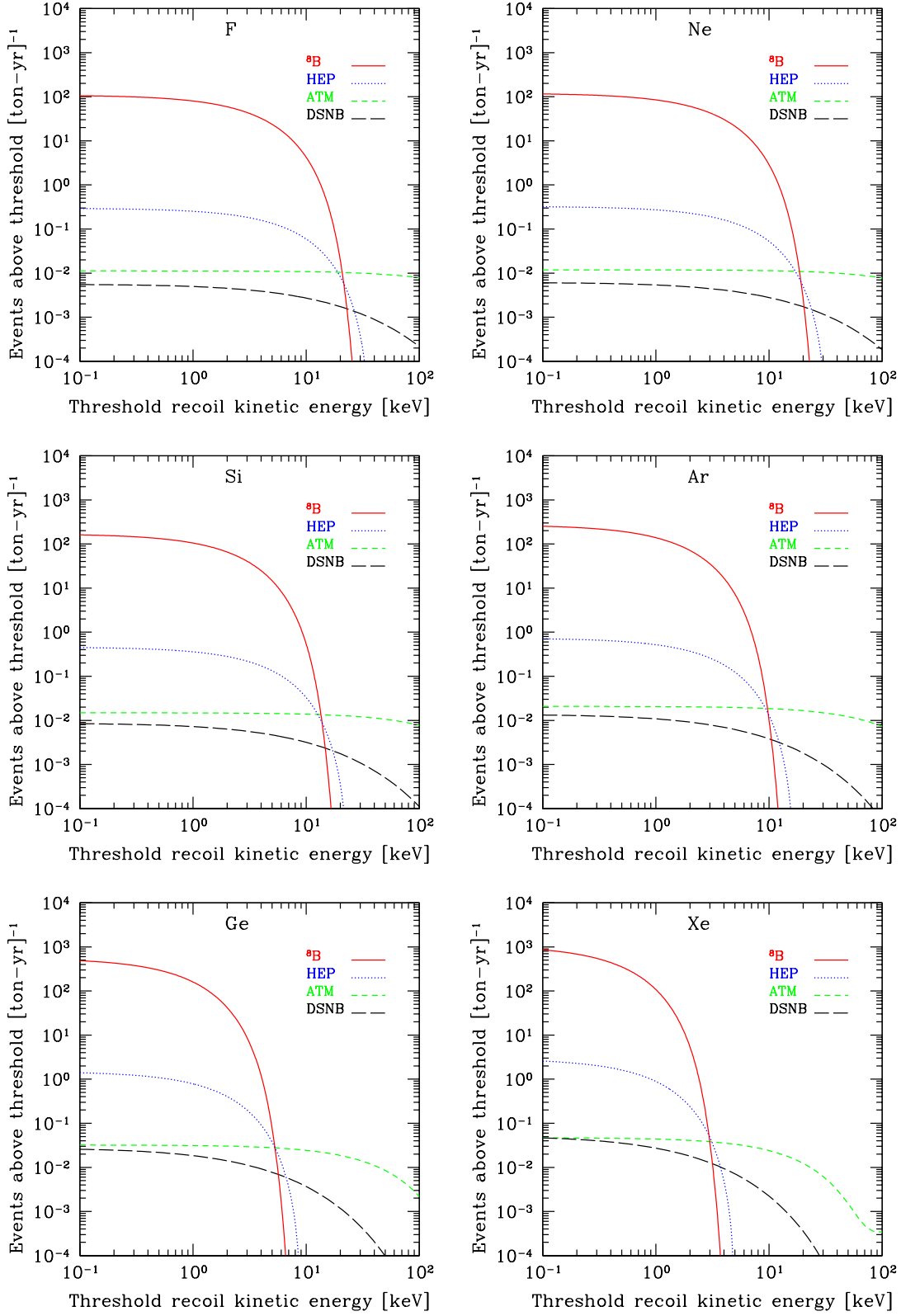
Figure 3. Number of events above a threshold recoil kinetic energy for six target nuclei. For both the diffuse supernova and atmospheric event rates, the sum of all contributing neutrino flavors are shown.

2.3. Event Rates

The differential event rate at a fixed recoil kinetic energy is

$$\frac{dR(T)}{dT} = \int_{E_{\min}}^{\infty} \frac{dN}{dE_\nu} \frac{d\sigma(E_\nu, T)}{dT} dE_\nu, \tag{3}$$

where dN/dE_ν is the neutrino flux spectrum and $E_{\min} = \sqrt{MT/2}$ is the minimum neutrino energy for a given recoil energy as dictated by the kinematics. Figure 2 shows the event rate recoil spectrum for six different nuclear targets. For all targets the naturally-occurring abundances are assumed. For both the diffuse supernova and atmospheric event rates, the sum of all contributing neutrino flavors are shown. In particular for the *DSNB*, an 8 MeV spectrum from Figure 1 is multiplied by four to account for the production spectrum of the four ν_x flavors. Due to their relatively hard spectra, the ν_x flavors are seen to dominate the event rate, particular at high recoil energies; there is only about a $\sim 10\%$ increase by including the 3 and 5 MeV spectra at the lowest recoil energies. Each of these curves are the true, infinite resolution spectra, i.e. they do not account for the expected finite energy resolution of detectors. A detailed convolution with a resolution function will depend on the nuclear target and the particular experimental environment.

Figure 3 shows the number of events above a given recoil energy for the same six nuclear targets. Most of the ^{8}B events are confined to low recoil energies, for example for the case of Xe there are a total of $\sim 10^3$ events over all energies, but only ~ 1 event per ton-yr above a threshold of 3 keV. Future Xe detectors are expected to have thresholds in the area of ~ 5 keV; as is seen dropping the threshold below this energy will lead to a significantly increased ^{8}B signal.

As an additional note, the analysis above just accounts for neutrino-nucleus coherent scattering. In principle it would also be possible to detect these same fluxes via neutrino-electron elastic scatterings [8]. For this channel the largest rate is to due the solar *pp* reaction. For example, from *pp* scatterings on Xe a flat spectrum of electron recoil events is expected at ~ 0.1 events per ton-yr with energies up to ~ 600 keV.

3. Implications for WIMP-Nucleon Cross Section Constraints

In the absence of backgrounds the expected upper limit on the WIMP-cross section simply scales linearly with the detector. For example a ten times greater exposure will imply a ten times stronger upper limit on the cross section. In the presence of backgrounds, however, the projected limits on the cross section must be modified. Dodelson [28] has provided a simple formalism for estimating the upper limit on the WIMP-nucleon cross section, given a measured background rate and a fiducial detector volume. In this formalism, the probability of observing a total of N events, given a WIMP-nucleon cross section, σ, is

$$\mathcal{L}(N|\sigma) \propto \int_0^{\infty} dN_b \exp\left[\frac{-(N_b - \bar{N}_b)^2}{2\sigma_b^2}\right] \frac{e^{-\mu}\mu^N}{N!}. \tag{4}$$

Here the mean, μ, is a sum of the WIMP-induced signal and neutrino-induced background events, and depends on the model parameters such as σ and the expected background spectrum. The mean number of background events is $\bar{N}_b$ and the error on the background is σ_b. In Eq. 4 the effect of binning the data in energy is neglected, and as a result the estimates quoted are likely to be conservative (binning the data would likely increase the sensitivity).

From the likelihood in Eq. 4, Dodelson [28] defines the *Background Penalty Factor* (*BPF*) as

$$\sigma_{\text{future}}^{\text{upper limit}} = \frac{\sigma_{\text{current}}^{\text{upper limit}}}{\lambda} \times BPF, \tag{5}$$

where λ is the ratio of the future detector exposure to the current exposure. The *BPF* then essentially measures, for a given background rate, the projected upper limit on the cross section for a future detector. It is calculated by integrating the normalized version of Eq. 4 up to the desired confidence level, and the projected cross section upper limit is then obtained from Eq. 5. Here the projected upper limits are quoted at 95% c.l.

The results presented here assume that the mean background event rates $\bar{N}_b$ are obtained from the results in the figures above. The error on the background is taken to be $\sigma_b = 0.2\bar{N}_b$, motivated by the uncertainty on the solar neutrino fluxes [29]. The results presented here are found to be independent of similar reasonable assumptions for the error on the background. As far as the actual measured backgrounds are concerned, recent results of XENON10 [2] and CDMS [3] give background rates per unit volume of (7 events)/(0.44 kg-yr) and (0.6 events)/(0.33 kg-yr), respectively. These backgrounds are not accounted for in this present analysis, amounting to the assumption that they can be reduced and understood in future experimental analysis. The calculations above show that, given the current exposures, the total background rate from all neutrino sources is $\sim 10^{-4}$ events above CDMS and XENON10 thresholds, so it is unlikely that these background events are neutrino-induced.

Accounting for the neutrino backgrounds, Figure 4 shows the upper limit on the cross section attainable as a function of detector exposure. Two target nuclei are considered, Xe and Ge. To set the absolute scale, the current WIMP-nucleon cross section upper limits from these experiments are $\sim 4 \times 10^{-44}$ cm^2 (at ~ 30 GeV) and $\sim 5 \times 10^{-44}$ cm^2 (at ~ 60 GeV), respectively [2, 3]. Each target shows the results for three different energy thresholds. The salient point is that, as the threshold is increased, the dominant ^{8}B background is reduced and the projected upper limit on the cross section will become much more stringent. In fact, cutting out the ^{8}B signal entirely (which amounts to adopting the 5 keV threshold for Xe and the 7 keV threshold for Ge), the projected upper limit will continue to decrease to below $\sim 10^{-12}$ pb, the lower regime of the supersymmetric model parameter space [4].

It should be noted that, while effective at eliminating backgrounds, setting the threshold at too high of an energy may have the adverse effect of cutting out the sought after signal events from WIMP-induced recoils. For example, for a 100 GeV WIMP, $\sim 10\%$ of the recoil events occur in energy bins below 3 keV. Similarly for a 50 GeV

WIMP, $\sim 15\%$ of the events occur in energy bins below 3 keV. So setting the threshold to cut the entire ^{8}B rate may not be the optimal strategy, depending on the underlying WIMP parameters. In this sense, determining the WIMP signal robustly will require a multi-component fit to both the WIMP and neutrino-induced recoil spectra.
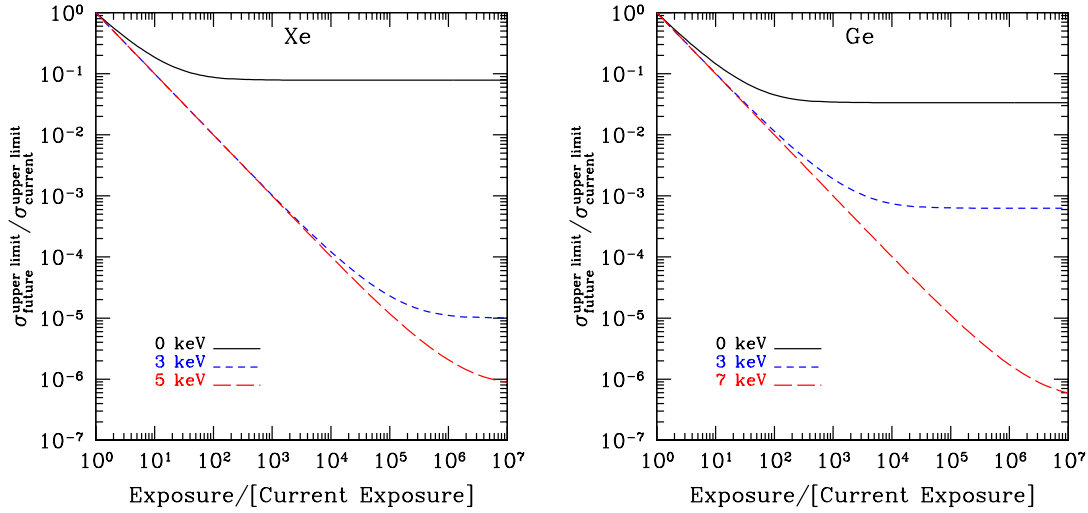

Figure 4. The upper limit on the WIMP-nucleon cross section, relative to the current upper limit, as a function of the exposure, relative to the current exposure. Two target nuclei are shown, Xe and Ge. The labels in each case denote the lower energy threshold assumed for the experiment. It is assumed that there are no non-neutrino sources contributing to the background.

4. Upper DSNB flux limit on non-electron neutrino flavors

The preceding section has discussed the extent to which the neutrino backgrounds can degrade the upper limits on the WIMP-nucleon cross section. It is also of course interesting to explore the neutrino fluxes in the context of a signal themselves. The focus here is on the *DSNB* flux, and more specifically to provide an estimate for the expected flux limit that current detectors can set on the ν_x flux component. Similar to the preceding section, the projections focus on Xe and Ge targets, though they can easily be extended to other targets with similar results.

From Figure 3, the expected *DSNB* event rate is ~ 0.05 events per ton-yr. As discussed above, this event rate is dominated by the four ν_x flavors, again not accounting for neutrino mixing. It follows that the detection of this flux requires an exposure of the order 100 ton-yr. To set the current scale, given that the current exposure for Xe is 0.44 kg-yr, the expected number of *DSNB* events is a paltry $\sim 2 \times 10^{-5}$.

Nonetheless, from these predicted event rates an estimate of the flux upper limit that present detectors can set may be obtained by simply increasing the flux normalization so that $\mathcal{O}(1)$ event would be expected in detectors with the present

exposures. The implied increase in the flux normalization is $\sim 1/(2 \times 10^{-5}) = 5 \times 10^4$. Given that the current best estimates for the *DSNB* flux are ~ 10 cm^{-2} s^{-1} for non-electron flavors (again not accounting for neutrino mixing effects), it is projected that, with current exposures, the ν_x upper flux limit will be reduced by more than an order of magnitude, so that the projected upper flux limit is

$$\phi_{\nu_x}^{\text{limit}} \lesssim 10^6 \, \text{cm}^{-2} \, \text{s}^{-1}. \tag{6}$$

This limit is valid for all energies, so in this way it is better than an order of magnitude greater than the Mt. Blanc flux limit, which is only valid for neutrino energies $\gtrsim 20$ MeV.

The flux upper limit in Eq. 6 may be viewed as optimistic, because no contaminating backgrounds in the energy window of the *DSNB* signal have been accounted for. Accounting for the current backgrounds may somewhat degrade this limit, though as in the preceding section it is assumed that these backgrounds can be eliminated in future runs of the experiment. Going further and pushing the flux sensitivity even lower requires subtracting the solar and atmospheric backgrounds. In fact, in order to determine how much better the flux limit in Eq. 6 will get as a function of detector exposure, it is possible to again appeal to the *BPF* formalism from the previous section. The only difference is that $\phi_{\nu_x}^{\text{limit}}$ replaces the cross section as the quantity to constrain.

Under the assumptions above the projected upper limits on the *DSNB* flux are obtained simply by reading off the limits from the curves in Fig. 4. Since the *DSNB* constitutes a small fraction of the total backgrounds in Fig. 4, it is found that calculating the flux limit in this manner provides an excellent approximation to the case in which the curves in Fig. 4 are calculated *without* the *DSNB* flux included. To set the normalization, the current flux limit is taken to be the projected value of $\phi_{\nu_x}^{\text{limit}}$ from Eq. 6. For a 0 keV threshold using an Xe target, from Fig. 4 the upper flux limit is projected to be reduced by about an order of magnitude further to $\lesssim 10^5$ cm^{-2} s^{-1} for a two order of magnitude increase in exposure. This scaling is again primarily because of the ^{8}B solar neutrino background. Eliminating the ^{8}B background with an energy threshold cut, Fig. 4 shows that the flux sensitivity will increase linearly with exposure down to the projected *DSNB* flux window of ~ 10 cm^{-2} s^{-1} for exposures $\sim 10^5$ times the current exposures.

Finally, it should be noted again that as in the case for the projected cross section limits, the *DSNB* flux estimates have not accounted for the detailed spectral shape of the signal or backgrounds. Only the energy threshold has been varied to eliminate the dominant ^{8}B background. Future detectors, with orders of magnitude more exposure than at present should be able to improve on the upper limits provided here by using the difference between the spectral shapes of the signal and background.

5. Discussion and Conclusion

This paper has discussed the neutrino-induced recoil spectrum at dark matter detectors due to solar, atmospheric, and diffuse supernova neutrinos. It is shown that ton-scale

detectors can expect ~ 100 ^{8}B neutrino events per ton year over all recoil energies. The dominant ^{8}B signal can be excluded using either spectral information or by an energy threshold cut. It should also be noted that the ^{8}B signal could be cleanly identified by a detector with directional sensitivity [30].

The effect of these neutrino-incuded recoils on the extraction of an upper limit on the WIMP-nucleon cross section has been examined. If the ^{8}B signal can be excluded, and for the particular case of Xe and Ge targets, the upper limit on the cross section is projected to scale linearly with the detector exposure. Non- ^{8}B backgrounds only impact the WIMP-nucleon cross section upper limit if the cross section is below $\sim 10^{-12}$ pb.

Acknowledgments

[1] G. Jungman, M. Kamionkowski, and K. Griest. Supersymmetric dark matter. *Phys. Rept.*, 267:195–373, 1996.

[2] J. Angle et al. Limits on spin-dependent WIMP-nucleon cross-sections from the XENON10 experiment. *Phys. Rev. Lett.*, 101:091301, 2008.

[3] Z. Ahmed et al. A Search for WIMPs with the First Five-Tower Data from CDMS. *arXiv:0802.3530*, 2008.

[4] L. Roszkowski, R. Ruiz de Austri, and R. Trotta. Implications for the Constrained MSSM from a new prediction for b to s gamma. *JHEP*, 07:075, 2007.

[5] S. Yellin. Finding an upper limit in the presence of unknown background. *Phys. Rev.*, D66:032005, 2002.

[6] D. Z. Freedman. Coherent neutrino nucleus scattering as a probe of the weak neutral current. *Phys. Rev.*, D9:1389–1392, 1974.

[7] K. Scholberg. Prospects for measuring coherent neutrino nucleus elastic scattering at a stopped-pion neutrino source. *Phys. Rev.*, D73:033005, 2006.

[8] B. Cabrera, L. M. Krauss, and F. Wilczek. Bolometric Detection of Neutrinos. *Phys. Rev. Lett.*, 55:25, 1985.

[9] J. Monroe and P. Fisher. Neutrino Backgrounds to Dark Matter Searches. *Phys. Rev.*, D76:033007, 2007.

[10] J. D. Vergados and H. Ejiri. Can Solar Neutrinos be a Serious Background in Direct Dark Matter Searches? *Nucl. Phys.*, B804:144–159, 2008.

[11] D. Z. Freedman, D. N. Schramm, and D. L. Tubbs. The Weak Neutral Current and Its Effects in Stellar Collapse. *Ann. Rev. Nucl. Part. Sci.*, 27:167–207, 1977.

[12] J. D. Lewin and P. F. Smith. Review of mathematics, numerical factors, and corrections for dark matter experiments based on elastic nuclear recoil. *Astropart. Phys.*, 6:87–112, 1996.

[13] J. N. Bahcall. *Neutrino astrophysics.* Cambridge and New York, Cambridge University Press, 1989, 584 p., 1989.

[14] T. K. Gaisser and M. Honda. Flux of atmospheric neutrinos. *Ann. Rev. Nucl. Part. Sci.*, 52:153–199, 2002.

[15] G. Battistoni, A. Ferrari, T. Montaruli, and P. R. Sala. The atmospheric neutrino flux below 100-MeV: The FLUKA results. *Astropart. Phys.*, 23:526–534, 2005.

[16] S. Horiuchi, J. F. Beacom, and E. Dwek. The Diffuse Supernova Neutrino Background is detectable in Super-Kamiokande. *arXiv:0812.3157*, 2008.

[17] M. Th. Keil, G. G. Raffelt, and H.-T. Janka. Monte Carlo study of supernova neutrino spectra formation. *Astrophys. J.*, 590:971–991, 2003.

[18] M. Malek et al. Search for supernova relic neutrinos at Super- Kamiokande. *Phys. Rev. Lett.*, 90:061101, 2003.

[19] B. Aharmim et al. A search for neutrinos from the solar hep reaction and the diffuse supernova neutrino background with the sudbury neutrino observatory. *Astrophys. J.*, 653:1545–1551, 2006.

[20] J. F. Beacom and L. E. Strigari. New test of supernova electron neutrino emission using Sudbury Neutrino Observatory sensitivity to the diffuse supernova neutrino background. *Phys. Rev.*, C73:035807, 2006.

[21] C. Lunardini. The diffuse neutrino flux from supernovae: Upper limit on the electron neutrino component from the non-observation of antineutrinos at superKamiokande. *Phys. Rev.*, D73:083009, 2006.

[22] A. G. Cocco, A. Ereditato, G. Fiorillo, G. Mangano, and V. Pettorino. Supernova relic neutrinos in liquid argon detectors. *JCAP*, 0412:002, 2004.

[23] M. Aglietta et al. Limits on low-energy neutrino fluxes with the Mont Blanc liquid scintillator detector. *Astropart. Phys.*, 1:1–9, 1992.

[24] C. Lunardini and O. L. G. Peres. Upper limits on the diffuse supernova neutrino flux from the SuperKamiokande data. *JCAP*, 0808:033, 2008.

[25] C. J. Horowitz, K. J. Coakley, and D. N. McKinsey. Supernova observation via neutrino nucleus elastic scattering in the CLEAN detector. *Phys. Rev.*, D68:023005, 2003.

[26] D. S. Akerib et al. Deep Underground Science and Engineering Lab: S1 Dark Matter Working Group. *astro-ph/0605719*, 2006.

[27] J. F. Beacom, W. M. Farr, and P. Vogel. Detection of supernova neutrinos by neutrino proton elastic scattering. *Phys. Rev.*, D66:033001, 2002.

[28] S. Dodelson. Backgrounds and Projected Limits from Dark Matter Direct Detection Experiments. *arXiv:0812.0787*, 2008.

[29] J. N. Bahcall and M. H. Pinsonneault. What do we (not) know theoretically about solar neutrino fluxes? *Phys. Rev. Lett.*, 92:121301, 2004.

[30] S. Henderson, J. Monroe, and P. Fisher. The Maximum Patch Method for Directional Dark Matter Detection. *Phys. Rev.*, D78:015020, 2008.